

AperTO - Archivio Istituzionale Open Access dell'Università di Torino

**A general strategy for the obtainment of biodegradable polymer shelled microbubbles as
theranostic device**

This is the author's manuscript

Original Citation:

Availability:

This version is available <http://hdl.handle.net/2318/120550> since 2016-10-10T16:06:23Z

Terms of use:

Open Access

Anyone can freely access the full text of works made available as "Open Access". Works made available under a Creative Commons license can be used according to the terms and conditions of said license. Use of all other works requires consent of the right holder (author or publisher) if not exempted from copyright protection by the applicable law.

(Article begins on next page)

This is the author's final version of the contribution published as:

Sabrina Capece; Ester Chiessi; Roberta Cavalli; Dmitry Grishenkov; Gaio Paradossi. A general strategy for the obtainment of biodegradable polymer shelled microbubbles as theranostic device. *CHEMICAL COMMUNICATIONS*. 49 pp: 5763-5765.

When citing, please refer to the published version.

Link to this full text:

<http://hdl.handle.net/2318/120550>

A general strategy for the obtainment of biodegradable polymer shelled microbubbles as theranostic device.

Sabrina Capecea, Ester Chiessia, Roberta Cavallib, Pierangela Giustettoc, Dmitry Grishenkod, and Gaio Paradossia, *

Fabrication of multifunctional ultrasound contrast agents (UCAs) have been recently addressed in several research groups. A versatile strategy for the synthesis of UCAs precursors in the form of biodegradable vesicles with a crosslinked biocompatible polymer is described. Upon ultrasound irradiation, acoustic droplet evaporation transforms such particles into microbubbles behaving as UCAs. This proof of concept entails the features of a potential theranostic microdevice.

The use of contrast media in medical imaging is increasing and new or revised devices are designed to implement their functionality. Microbubbles (MBs) are used as ultrasound contrast agent (UCA).¹ They are micron-sized systems consisting of a gas core stabilized by a lipid or polymeric shell. Advantages and disadvantages are present in the use of both types.² Lipid shelled MBs scatter ultrasound efficiently but, once injected, their life in the blood pool is quite short and their dimensions are characterized by a broad distribution. Chemical modifications of the lipid layer have been attempted in order to target MBs to pathological tissues or cells.³ Polymer shelled MBs are more stable.⁴ However, their shell is less elastic than the lipidic ones, causing a lower echogenicity. The robustness of their shell is an asset if extensive chemical modifications are planned to enable multimodal imaging in combination with targeting and drug delivery capabilities. Surface decoration represents a step further toward the design of a truly theranostic device.⁵

Design of multimodal contrast agents, enabling a limited number of functionalities can be easily found in the literature.⁶ Recently, Rapoport⁷ described the method for depositing a polymer layer using a PFC-in-water miniemulsion stabilized by an amphiphilic co-polymer. To obtain polymer shelled nanocapsules, Cavalli⁸ layered chitosan on perfluorocarbon nanodroplets stabilized by the presence of an emulsifying agent.

In this paper we describe a general, robust strategy for the obtainment of MBs with different crosslinked polymer shells. Fig. 1 shows a schematic representation of the assembly process involving (i) the deposition of a shell of a surfactant layer, around a PFC, typically decafluoropentane, droplet in water; (ii) the deposition, as outmost layer on the water/vesicle interface, of a hydrophilic polymer grafted with a vinyl moiety, driven by the ability of the vinyl residues to stick in the vesicle shell; (iii) the free radical photopolymerization to crosslink the grafted vinyl side-chains. The interfacial properties of PFCs are unique and the use of these compounds can be advantageously exploited for pharmaceutical formulations.^{1,9,10} Polysaccharides bearing hydrophobic methacrylate side chains spontaneously accommodate on top of the surfactant shell to form the outer polymer layer.

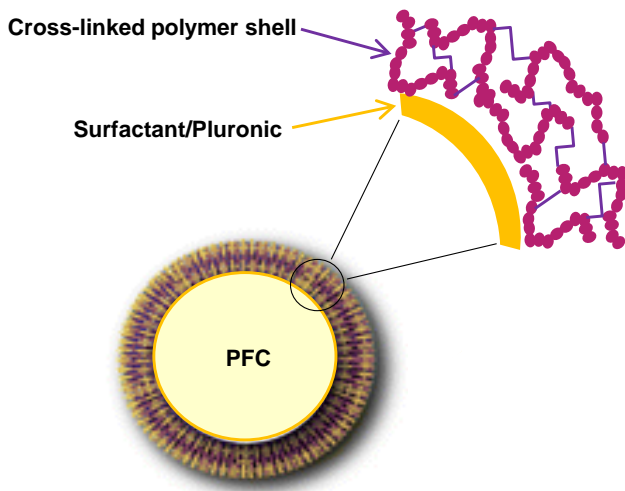


Fig. 1 Schematic representation of polymer shelled vesicles.

The polymerization is then triggered by a photoinitiator and the polysaccharide shell is crosslinked around the PFC liquid core. These vesicles, irradiated by ultrasound (US), can undergo an acoustic droplet vaporization, ADV,¹¹ which allows a liquid \rightarrow gas transition in the core, transforming the polymer vesicles into MBs. This process is readily observed by the floating tendency of the MBs and can be monitored by laser scanning confocal microscopy (CLSM), coupling rhodamine B isothiocyanate, RBITC, on the polymer shells. In CLSM images the vesicles/microbubbles are described as rings after focusing the equatorial plane of fluorescent labelled shells.

As candidates for the fabrication of the shell, we have explored the properties of methacryloyl-grafted dextran and hyaluronic acid. Both polysaccharides are biodegradable¹² and their degree of substitution, DS, is 50 and 30 % (mol/mol), respectively. These polymers will be named hereafter DexMA50 and HAMA30, respectively. Methacrylic moiety is readily photopolymerized in emulsion, forming poly(methacrylic), pMA, chains. In this way the grafted polymers are crosslinked in a network constituting the shell of the vesicle.¹³

The synthesis of such derivatives and that of the polymer shelled vesicles are reported in the supporting information. Fig. 2 highlights the behaviour of DexMA50 vesicles upon treatment with US with characteristics reported in the supporting information.

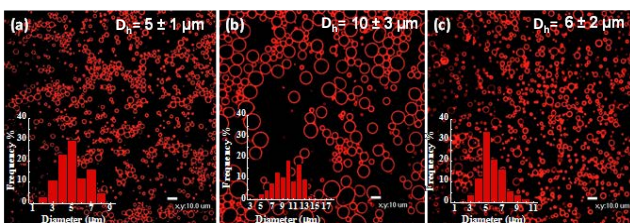


Fig. 2 Confocal microscopy of DexMA50 shelled vesicles (a) before US irradiation, (b) after US irradiation and (c) one hour after US irradiation. Insets: size distributions and mean diameters.

Before US irradiation (Fig. 2, a), the vesicles sink in water because of the higher density of the liquid decafluoropentane core. Their average diameter is 5 μm . After US irradiation (Fig. 2, b), the energy provided under the form of ultrasound mechanical waves enables the transition of the liquid PFC to gas and the passage from vesicles to MBs with a marked increase of the average diameter of about 5 μm . Once the energy has been dissipated (Fig. 2, c), the MBs revert to vesicles recovering the original diameter. In an ideal bubble, with infinitely thin shell having a surface tension σ and a radius r , the inside pressure, P_{in} , is equal to the outside pressure, P_{out} , increased by the Laplace pressure term:

The boiling point of decafluoropentane at standard pressure is 55 $^{\circ}\text{C}$ with a vaporization enthalpy of 6816 cal/mol.¹⁴ The additional Laplace term increases the boiling point of the liquid core well above the physiological temperature.¹⁵ The action of the US is key for the vaporization and it is showed in DexMA50 MBs by a 100 % of increase in the system dimensions. This change depends on the polymer elasticity and on the crosslinking degree of the shell. The reported behaviour opens a future perspective in the exploitation of the vesicle \square microbubble transition for a combined imaging and therapeutic approach. The liquid hydrophobic core can be regarded as a drug reservoir to be targeted in the vicinity of the pathological tissue and, via US driven ADV, simultaneously allowing the sonographic imaging. MBs can be blasted, if properly excited by US, to release the drug payload. The US conditions in which DexMA50 MBs can be destroyed in an in vitro experiment is reported in supporting information.

DexMA50 MBs echogenicity was tested in an in vitro experiment using either 18 or 24 MHz transducers of a Vevo2100 (VisualSonics Inc.) instrument, which provides high resolution imaging down to 30 microns and non-linear image analysis. Two acquisition modalities are captured: traditional B - mode and non-linear contrast modality.¹⁶

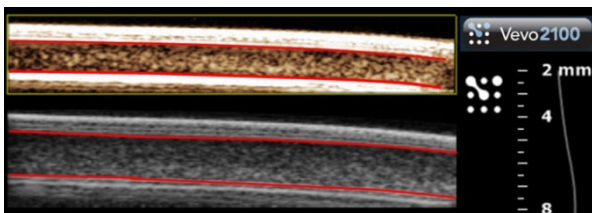


Figure 3 – DexMA50 MBs images acquired with the Vevo 2100 system using a 18 MHz probe and power level set to 100%. Top: non-linear mode. Bottom: traditional B-Mode. The red lines help to identify the inner walls of the silicon tubes.

The experimental details are described in the supporting information. A good echogenicity is found (Fig. 3). MBs are clearly visible in the tube lumen, with more intense echo signals in the non-linear image modality. The peak of negative pressure value at which ADV transition occurs is about 1 MPa, according to a

harmonic analysis, is shown in Figure 4. 1MPa corresponds to a mechanical index, MI, of 0.67, a value well below 1.9 indicated as the safety limit of medical ultrasound scanners. Experimental details are reported in supporting information.

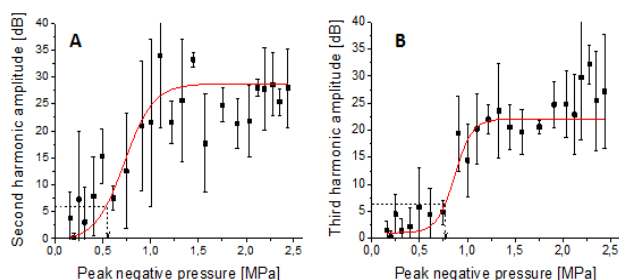


Fig. 4 Second (A) and third (B) harmonic amplitude as a function of applied negative pressure.

The biodegradation is a key issue for the drug delivery and for assessing the bioelimination pathways, usually involving spleen or liver. Fig. 5 shows that dextran shelled MBs are degraded by the catalytic action of lysozyme. In the presence of a more specific enzyme such as dextranase, the degradation time is much shorter (see supporting information for details).

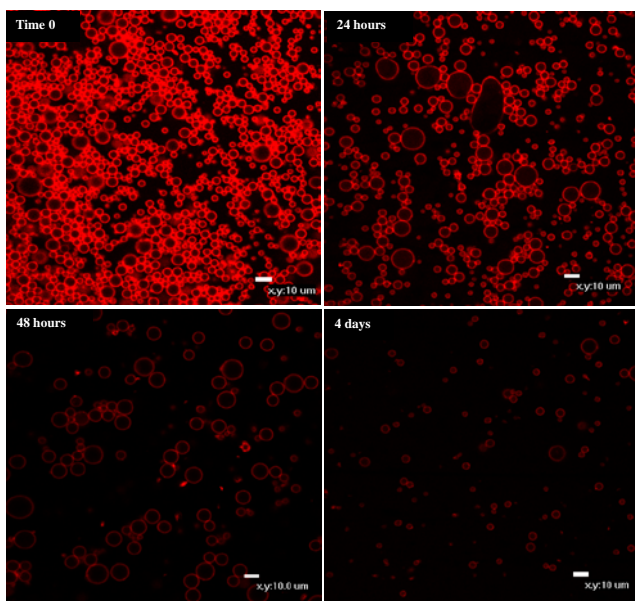


Fig. 5 Lysozyme catalysed degradation of DexMA50 vesicles.

To demonstrate the effective versatility of this synthetic route, an additional vinyl monomer, N-isopropylacrylamide (NiPAAm), was added to the MB shells and co-polymerized with the methacrylic sidechains of the grafted dextran. In this case, dextran chains are crosslinked by poly(methacrylate-co-NiPAAm) co-polymer chains, with the inclusion in the shell of random sequences of NiPAAm. This residue is often used as co-monomer to add thermal responsivity to a polymer due to the lower critical solution temperature (LCST) present in oligomers and polymers.¹⁷ Vesicles shells containing dextran crosslinked to p(methacrylate-co-NiPAAm), dex/p(MA-co-NiPAAm), have a thermoresponsive behaviour, as highlighted in Fig. 6.

When the temperature is increased from 25 to 45 °C, the fluorescence of dex/p(MA-co-NiPAAm) vesicles is quenched almost completely. On cooling back to RT, the vesicles emit fluorescence as in the starting conditions, indicating the absence of MB degradation occurring during the heating step. In a control experiment, DexMA50 shelled vesicles do not show a fluorescence quenching when heated at 45 °C (Fig. 6, b').

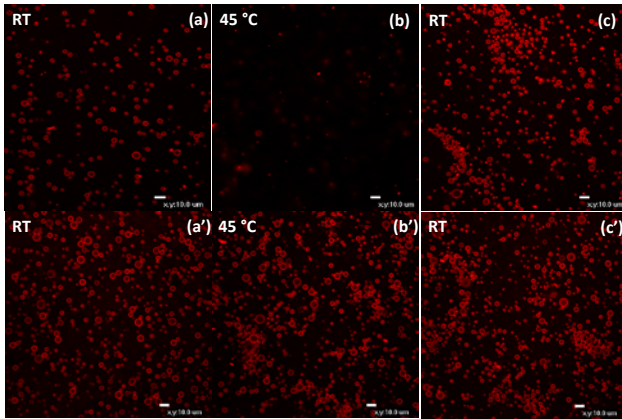


Fig. 6 Thermal behaviour of dextran based vesicles: dex/p(MA-co-NiPAAm) shelled vesicles. (a) at room temperature (RT); (b) at 45 °C; (c) back at RT; DexMA50 shelled vesicles (d) at RT; (e) at 45 °C and (f) back at RT.

We hypothesize that the quenching of fluorescence in the NiPAAm containing vesicles at 45 °C is due to an LCST effect localized in the vesicle shells, which shields the fluorophore from the incident light decreasing substantially the fluorescence emission.¹⁸

With small changes with respect to the synthesis of DexMA50 vesicles, vesicles can be fabricated with methacrylate derivative of hyaluronic acid having a degree of substitution of 30 %, HAMA30. The droplets of liquid PFC were stabilized with Pluronic 127 and octylamine as co-surfactant. Details of the synthesis are reported in the supporting information. The positive charges on octylamine favour the deposition of HAMA30 on the surface of the surfactant layer. The behaviour upon US irradiation is quite similar to what found for DexMA50 MBs. The increase in the diameter following US irradiation is about 100 % (see Figure 7).

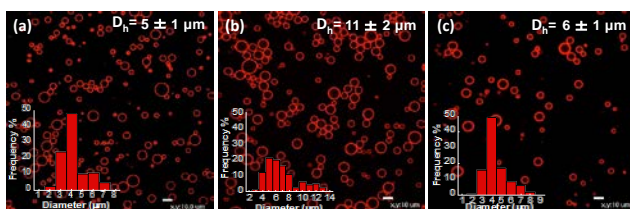


Fig. 7 Confocal microscopy of HAMA30 shelled vesicles (a) before US irradiation, (b) after US irradiation and (c) one hour after US irradiation. Insets: size distributions and mean diameters.

Conclusions

We have presented a new class of core-shell microsystems based on biodegradable crosslinked polymers with features that can be exploited for the design of a multifunctional device. The micron size of these vesicles makes easier the ADV as compared to nanovesicles, allowing an easy US visualization. This unique

set of properties can be exploited for the design of a theranostic device with a potential huge impact on multimodality imaging and anticancer therapy. Moreover, peak negative pressure threshold values necessary to allow US imaging are compatible with the safety limits suggested by medical directories.

a Dipartimento di Scienze e Tecnologie Chimiche, Università di Roma Tor Vergata, Via della Ricerca Scientifica, 00133 Rome, Italy. Fax: +39 7259 4328; Tel: +39 7259 4464; E-mail: paradossi@stc.uniroma2.it

bDipartimento di Scienza e Tecnologia del Farmaco, Università di Torino, via P. Giuria 9, 10125 Torino, Italy

cUniversity of Torino, Department of Molecular Biotechnology and Health Sciences, Molecular Imaging Center - Torino, Italy and Center for Preclinical Imaging - Colleretto Giacosa (TO), Italy

d Division of Medical Engineering, School of Technology and Health, Royal Institute of Technology, KTH, Alfred Nobels allé 10, SE-141 52 Huddinge, Sweden

Notes and references

1. E. G. Shutt, D. H. Klein, R. M. Mattrey and J. G. Riess, *Angew. Chem. Int.*, 2003, 42, 3218.
2. E. C. Unger, T. Porter, W. Culp, R. Labell, T. Matsunaga and R. Zutshi, *Adv. Drug Del. Rev.*, 2004, 56, 1291.
3. J. J. Rychak, J. R. Lindner, K. Ley and A. L. Klibanov, *J. Controlled Release*, 2006, 114, 288;
4. F. Cavalieri, A. El Hamassi, E. Chiessi and G. Paradossi, *Langmuir*, 2005, 21, 8758.
5. (a) S. Fokong, B. Theek, Z. Wu, P. Koczana, L. Appold, S. Jorge, U. Rosch-Genger, M. van Zandvoort, G. Storm, F. Kiessling and T. Lammers, *J. Controlled Release*, 2012, 163, 75; (b) S. Hernot and A. L. Klibanov, *Adv. Drug Del. Rev.*, 2008, 60, 1153.
6. (a) B. Geers, H. Dewitte, S. C. De Smedt and I. Lentacker, *J. Controlled Release*, 2012, 164, 248. ; (b) T. B. Brismar, D. Grishenkov, B. Gustafson, J. Hamark, A. Barrefelt, S. V. V. N. Kothapalli, S. Margheritelli, L. Oddo, K. Caidhal, H. Hebert and G. Paradossi, *Biomacromol.*, 2012, 13, 1390.
7. N. Rapoport, K. H. Nam, R. Gupta, Z. Gao, P. Mohan, A. Payne, N. Todd, X. Liu, T. Kim, J. Shea, C. Scaife, D. L. Parker, E. K. Jeong and A. M. Kennedy, *J. Controlled Release*, 2011, 153, 4.
8. (a) R. Cavalli, A. Bisazza, M. Trotta, M. Argenziano, A. Civra and D. Lembo, *Int. J. Nanomedicine*, 2012, 7, 3309; (b) R. Cavalli, A. Bisazza, A. Rolfo, S. Balbis, D. Madonnaripa, I. Caniggia and C. Guiot, *Int. J. Pharm.*, 2009, 378, 215.
9. M. A. Kandadai, P. Mohan, G. Lin, A. Butterfield, M. Skliar and J. J. Magda, *Langmuir*, 2010, 26, 4655.
10. P. G. A. Rogueda, *Drug Dev. Ind. Phar.*, 2003, 29, 39.
11. O. D. Kripfgans, J. B. Fowlkes, D. L. Miller, O. P. Eldevik and P. L. Carson, *Ultrasound Med. Biol.*, 2000, 26, 1177.
12. (a) J. B. Leach, K. A. Bivers, C. W. Patrick Jr. and C. E. Schmidt, *Biotechnol. Bioeng.*, 2003, 82, 578; (b) O. Franssen, R. D. van Ooijen, D. de Boer, R. A. A. Maes and W. E. Hennink, *Macromol.*, 1999, 32, 2896.

13. (a) S. V. Ghugare, E. Chiessi, B. Cerroni, M. T. Telling, V. G. Sakai and G. Paradossi, *Soft Matter*, 2012, 8, 2494; (b) S. V. Ghugare, E. Chiessi, R. Fink, Y. Gerelli, A. Scotti, A. Deriu, G. Carrot and G. Paradossi, *Macromol.*, 2011, 44, 4470.
14. E. J. Barber and G.H. Cady, *J. Phys. Chem.*, 1956, 60, 504.
15. (a) P. S. Shereran, V. P. Wong, S. Luois, R. J. McFarland, W. D. Ross, S. Feingold, T. O. Matsunaga and P. A. Dayton, *Ultrasound Med. Biol.*, 2011, 37, 1518 ; (b) N. Rapoport, D. A. Christensen, A. M. Kennedy and K. Nam, *Ultrasound Med. Biol.*, 2010, 36, 419.
16. C. M. Moran, S. D. Pye, W. ellis, A. Janeczko, K. D. Morris, S. McNeilly and H. M. Fraser, *Ultrasound Med. Biol.*, 2011, 37, 493.
17. Y. Oho and T. Shikata, *J. Phys. Chem., B*, 2007, 111, 1511.
18. Y. Shirishi, R. Myamoto and T. Hirai, *J. Photochem. And Photobiol., A.*, 2008, 200, 432.